PCCP

PAPER

View Article Online
View Journal | View Issue

Cite this: *Phys. Chem. Chem. Phys.*, 2025, **27**, 7605

Color variation in radio-luminescence of P-dots doped with thermally activated delayed fluorescence molecules†

Zheming Su,‡[a] Hieu Thi Minh Nguyen, ‡[b] Zuoyue Liu,[a] Daiki Asanuma,[a] Minoru Yamaji, [c] Masanori Koshimizu, [d] Hajime Shigemitsu, [e] Sachiko Tojo,[a] Tadashi Mori, [e] Toshiyuki Kida, [e] Guillem Pratx, *[b] Mamoru Fujitsuka *[af] and Yasuko Osakada *[af]

Received 31st January 2025,
Accepted 18th March 2025

DOI: 10.1039/d5cp00410a

rsc.li/pccp

Thermally activated delayed fluorescence (TADF) materials possess exceptional photophysical properties. Organic scintillators utilizing TADF materials have shown great promise for applications requiring efficient radio-luminescence, owing to their high quantum efficiency and tunable emission properties. Previous studies demonstrated that polymer dots (**P-dots**) doped with TADF materials exhibit radio-luminescence under hard X-ray and electron beam excitation. However, the TADF materials used in these experiments were limited to limited color options, restricting their utility and hindering the exploration of multicolor radio-luminescence necessary for advanced applications. In this study, we successfully achieved multicolor radio-luminescence-blue, yellow, and red-by developing **P-dots** doped with TADF materials that emit across the visible spectrum. This breakthrough was demonstrated under excitation by hard X-rays, gamma rays, and electron beams. The ability to realize multicolor radio-luminescence is crucial, as it enables enhanced spatial and spectral resolution, which is vital for applications such as high-precision bio-imaging and multimodal sensing.

Thermally activated delayed fluorescence (TADF) molecules offer high quantum yields and long photoluminescence lifetimes without heavy metals, which is a considerable advantage for various applications in catalysis, optical devices, organic light-emitting diodes and bio-imaging.[1–3] These molecules use triplet excited state through reverse intersystem crossing to achieve efficient photo-luminescence, making them a promising alternative to conventional phosphorescent materials that rely on inorganic nanomaterials and metal complexes with heavy atoms.[4–7]

Recently, there has been considerable interest in developing radiation detection systems using TADF molecules, particularly in the form of scintillators.[8,9] Although most scintillators used for imaging, PDT, and other biological applications are often composed of inorganic materials, these materials present challenges such as limited tenability in colors and potential biocompatibility issues.[10–12] TADF-molecule based scintillators also emit light when exposed to ionizing radiation, and their use in imaging and sensing applications has been expanding owing to their high sensitivity and fast response times. Therefore, these advantages highlight the potential of TADF molecules in advancing next-generation, multi-color radiation detection tools.[13–16]

Our previous research demonstrated that polymer dots (**P-dots**) doped with TADF molecules exhibited blue radio-luminescence when exposed to hard X-rays and an electron beam.[17] This finding highlights the potential of TADF-doped **P-dots** as scintillating materials for radiation detection. However, previous investigations have been limited to a single emission color, specifically blue light. This color limitation restricts the scope of applications that require diverse color emissions for improved signal differentiation and imaging versatility. This limitation greatly hinders the broader applicability and

[a] *SANKEN (The Institute of Scientific and Industrial Research), Osaka University, Mihogaoka 8-1, Ibaraki, Osaka 567-0047, Japan. E-mail: yosakada@sanken.osaka-u.ac.jp, fuji@sanken.osaka-u.ac.jp*
[b] *Department of Radiation Oncology and Medical Physics, Stanford University, 3172 Porter Dr, Palo Alto, CA 94304, USA*
[c] *Division of Molecular Science, Graduate School of Science and Engineering, Gunma University, Ota, Gunma 373-0057, Japan*
[d] *Research Institute of Electronics, Shizuoka University, 3-5-1 Johoku, Naka-ku, Hamamatsu, 432-8011, Japan*
[e] *Department of Applied Chemistry, Graduate School of Engineering, Osaka University, 2-1 Yamadaoka, Suita, Osaka 565-0871, Japan*
[f] *Innovative Catalysis Science Division, Institute for Open and Transdisciplinary Research Initiatives (ICS-OTRI), Osaka University, 2-1 Yamadaoka, Suita, Osaka 565-0871, Japan*

† Electronic supplementary information (ESI) available. See DOI: https://doi.org/10.1039/d5cp00410a

‡ These authors contributed equally to this work.

potential for generating multi-color radio-luminescence, which could vastly enhance imaging and sensing capabilities.[18] Additionally, X-rays and gamma rays produce secondary electrons when they interact with materials. The process by which these secondary electrons lose energy produces scintillation light, so understanding the production and behaviour of electron beams is very important for improving the performance of scintillation materials.[15] Additionally, no quantitative measurements of scintillation properties, such as decay profiles, have been conducted with **P-dot** nanoscale scintillators for various types of radiation.[19]

In this study, we aimed to expand the understanding of the photochemical properties and radio-luminescence behavior of TADF doped **P-dots**. We explored various TADF molecules as dopants to achieve multicolor radio-luminescence and developed a versatile scintillating system capable of emitting multicolors under radiation, including electron beams, hard X-rays and gamma-rays.

Fig. 1 shows the conceptual diagram and molecular structures of the TADF molecules used in this investigation. Of previously reported TADF molecules, we selected three (**1** (DMAC-DPS),[20] **2** (4CzIPN),[21] **3** (oDTBPZ-DPXZ)[22]) that exhibit different emission wavelengths and photo-luminescence quantum yields of 50, 73, and 22% for **1**, **2** and **3** in toluene under argon, respectively) upon UV photoexcitation at 355 nm (Table S1, ESI†). In the early stages of the research, the three compounds in this study were selected by screening for quantum yields of luminescence greater than 20% and 50% for red and other colors, respectively. By using polyvinylcarbazole (PVK) and amphiphilic polyethylene glycol-COOH (PEG-COOH) polymers as carriers for these molecules, the **P-dots** were synthesized by the co-precipitation method previously described.[4,17] The formation of the **P-dots** was confirmed by transmission electron microscopy (TEM), which showed the

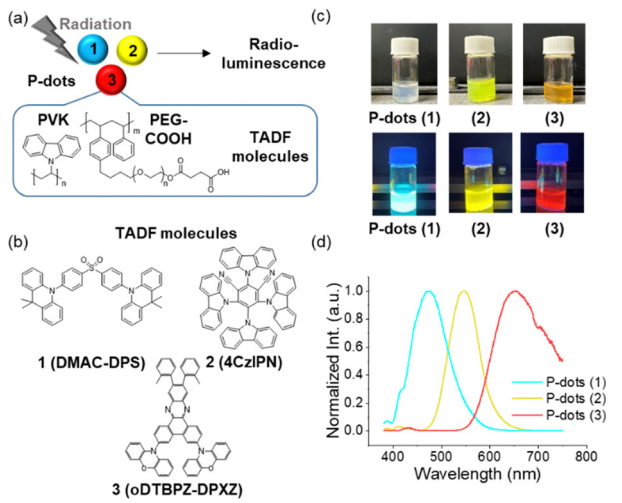

Fig. 1 (a) Conceptual diagram of TADF **P-dots** showing radio-luminescence exhibiting various colors. (b) Chemical structures of TADF molecules used in this study. (c) Photographs of **P-dots (1)**, **P-dots (2)** and **P-dots (3)** under room light (top) and ultra-violet light (365 nm) (bottom). (d) Normalized photoluminescence spectra of **P-dots (1)**, **P-dots (2)** and **P-dots (3)** excited at 355 nm.

formation of nanoparticles of 96, 88, and 95 nm in diameter for **P-dots (1)**, **P-dots (2)**, and **P-dots (3)**, respectively (Table S2, ESI†). A representative TEM image and a particle size distribution histogram are shown in Fig. S1 (ESI†). The size of each **P-dot** was also measured by dynamic light scattering, and the hydrodynamic diameters of **P-dots (1)**, **P-dots (2)**, and **P-dots (3)** was 142, 126, and 69 nm for respectively (Table S3, ESI†). These sizes are similar to those of the **P-dots** synthesized in previous studies.[17]

Upon UV excitation, the emission maximum wavelength was 475, 545, and 650 nm for **P-dots (1)**, **P-dots (2)**, and **P-dots (3)**; this sky blue, yellow, and red emission was confirmed visually (Fig. 1c, d, and Table 1). The emission wavelength maxima were 465, 510, and 600 nm, respectively, in toluene (Table S1, ESI†). A 10–50 nm red shifts was observed for each **P-dots** compared with the monomeric state (Fig. S2, ESI†). We checked the effect of doping concentration dependency on photoluminescence spectra (Table S4 and Fig. S3, ESI†). It is worth noting that the photoluminescence in **P-dots (1)** was greatly quenched, possibly derived from aggregation induced emission as suggested in EL efficiency.[23] Although there is a significant reduction in luminescence in **P-dots (1)**, from the perspective of application, the following experiments were conducted by comparing the same amount of doping in the three compounds. The photo-luminesces absolute quantum yields of the **P-dots** were not greatly affected by the presence of oxygen, as shown in Table 1, whereas those for the monomer molecules were reduced in the presence of molecular oxygen (Table 1). These results suggest that photo-luminescence in these **P-dots** is of moderate intensity and independent of oxygen (Table 2).

To investigate the photochemical properties of these multi-colored TADF **P-dots** in more detail, luminescence lifetime and transient absorption measurements were performed. First, the photo-luminescence lifetimes of the **P-dots** were examined in the presence and absence of molecular oxygen (Fig. 2).[24] The photo-luminescence lifetimes in the absence of molecular oxygen were 776, 24, and 47 ns for **P-dots (1)**, **P-dots (2)**, and **P-dots (3)**, respectively (Table S5, ESI†). Little oxygen-induced luminescence quenching, which was observed in monomer molecules in organic solvents, was observed with these **P-dots** (Fig. S4, ESI†). We also examined the effect of temperature on the luminescence lifetime, but within the range that could be measured, there was no significant difference, even though the solvent was water (Fig. S5, ESI†).

Next, transient absorption measurements were performed to directly observe the excited state dynamics and especially the effect of oxygen.[25] As with the luminescence lifetime results, no quenching of excited states due to oxygen was observed, but this was found for the monomer molecules in organic solvents (Fig. 3 and Fig. S6, S7 and Tables S6 and S7, ESI†). The triplet state spectra were also confirmed using electron beam excitation of the monomer in toluene by pulse radiolysis (Fig. S7, ESI†), while the spectra in toluene might not fully reflect the spectra in water. Although it is possible that using excitation light of 355 nm may cause a different electronic state to be excited throughout the system than radiation excitation, it is thought that there is no difference in the final emission

Table 1 Photoluminescence characteristics for TADF **P-dots**

Samples	λ_{max} [a] (nm)	FWHM (nm)	Φ_{PL} [b] (Ar)	Φ_{PL} [b] (Air)	Φ_{PL} (Air)/Φ_{PL} (Ar)	Φ_{PL} (**P-dots**)/Φ_{PL} (monomer)
P-dots (1)	475	89	0.28	0.33	1.18	0.56
P-dots (2)	545	71	0.21	0.18	0.86	0.29
P-dots (3)	650	133	0.05	0.04	0.80	0.23

[a] Photoluminescence λ_{max}. [b] Absolute quantum yields of photoluminescence.

Table 2 Triplet lifetime and reaction rate constant with molecular oxygen determined by laser flash photolysis

Samples	τ (μs, Ar)[a]	τ (μs, air)[a]	k_q (L mol^{-1} s^{-1})[b]
1	1.9	0.05	1.0×10^{10}
P-dots (1)	1.5	1.5	—
2	3.2	0.39	1.2×10^{9}
P-dots (2)	1.1	1.3	—
3	1.2	0.20	2.3×10^{9}
P-dots (3)	0.47	0.46	1.8×10^{8}

[a] Triplet lifetime and [b]Reaction rate constants determined by the equation of $k_{air} = k_{Ar} + k_q[O_2]$, $k_{air} = 1/\tau$ (air), and $k_{Ar} = 1/\tau$ (Ar). [b] Monomers were measured in toluene ($[O_2] = 1.8 \times 10^{-3}$ mol L^{-1}), and **P-dots** were measured in H_2O ($[O_2] = 2.9 \times 10^{-4}$ mol L^{-1}).

mechanism, which is emission from S1 state, and the results so far are important results for this research (Tables S6 and S7, ESI†). In any case, these results further confirm that encapsulation of TADF molecules into **P-dots** inhibits the diffusion reaction between the excited TADF molecule and molecular oxygen to quench the emission.

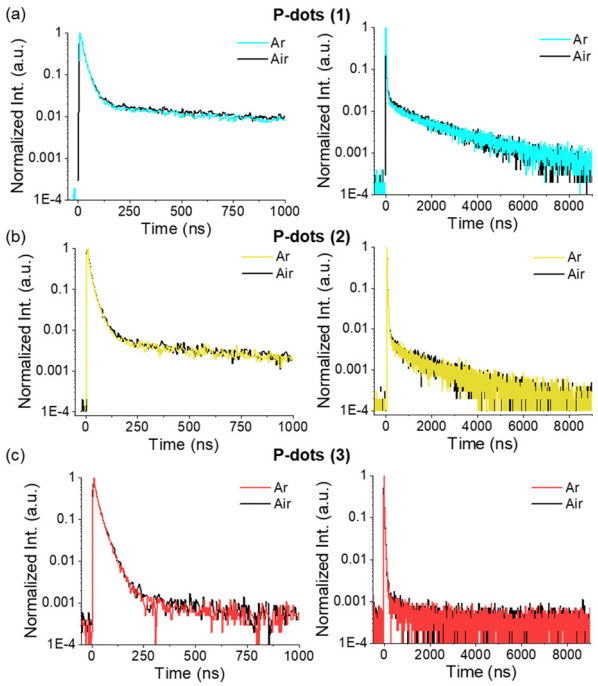

Fig. 2 Time-resolved photoluminescence decay curves for **P-dots (1)** (a), **P-dots (2)** (b), and **P-dots (3)** (c) in different timescales (left: 0–1000 ns, right: 0–9000 ns). Measurements taken under argon atmosphere are shown in color (sky blue, yellow, and red), while those taken in the presence of molecular oxygen are shown in black.

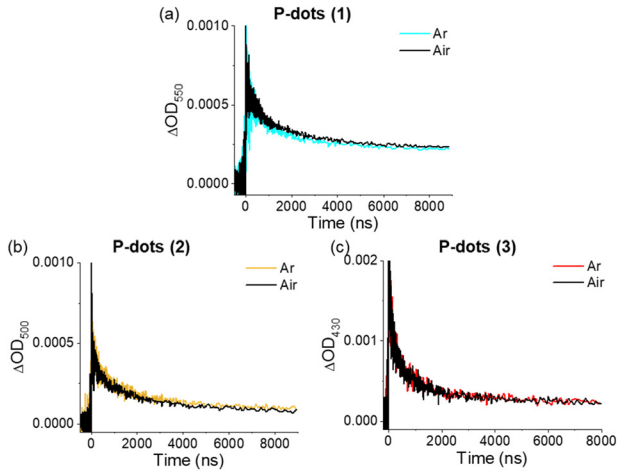

Fig. 3 Decay profiles of transient absorption for **P-dots (1)** (a) at 550 nm, **P-dots (2)** (b) at 500 nm, and **P-dots (3)** (c) at 430 nm excited at 355 nm. Measurements taken under argon atmosphere are shown in color (sky blue, yellow, and red), while those taken in the presence of oxygen are shown in black.

We explored the time-dependent scintillation intensity using time-correlated single photon counting of **P-dot** films upon gamma-ray excitation (Fig. 4).[26] Using a nuclide that emits multiple gamma rays simultaneously, the detection signal of one gamma ray was used as the timing signal and measured scintillation signal.[27] Although there are slight deviations due to

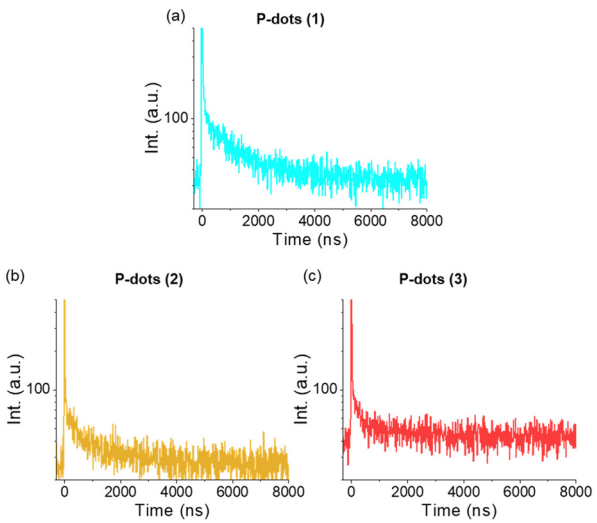

Fig. 4 Time dependence of scintillation intensity by gamma ray excitation for **P-dots (1)** (a), **P-dots (2)** (b), and **P-dots (3)** (c).

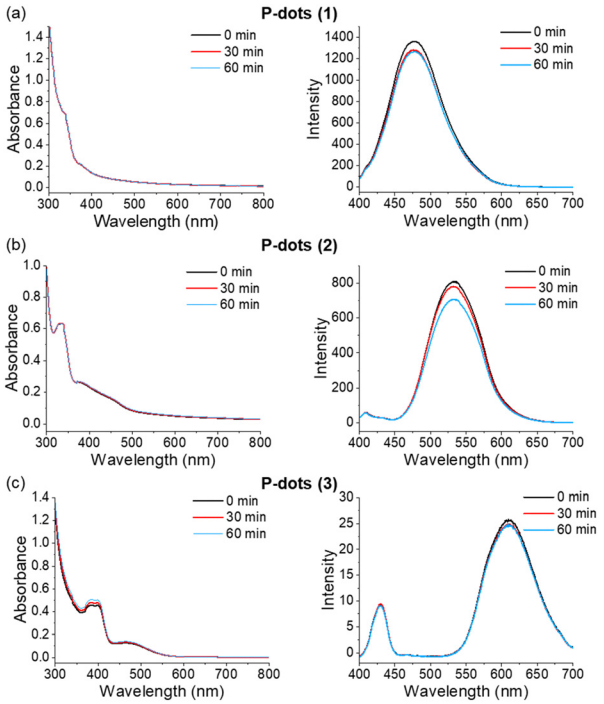

Fig. 5 Stability test upon gamma-ray irradiation. UV (Left) and emission spectra excited at 355 nm (right), before and after gamma ray irradiation for (a) **P-dots (1)**, (b) **P-dots (2)** and (c) **P-dots (3)** at a dose rate of 17.45 Gy h^{-1} from a distance of 1 m for 30 or 60 min.

differences in the time resolution of the measurement methods, the speed trends are generally consistent with the results of lifetime measurements by other methods (Table S8, ESI†). We also confirmed the stability of **P-dots** for gamma-ray irradiation. **P-dots** were irradiated with gamma-ray at a dose rate of 17.45 Gy h^{-1} from a distance of 1 m for 30 or 60 min. After the irradiation, the absorption and photoluminescence spectra (Fig. 5), and the size of **P-dots** were measured by DLS (Table S3, ESI†). There was no significant difference in the emission spectrum or size before and after irradiation. Therefore, we believe that the radiation induced chemistry would be excluded even under high radiation doses of 17 Gy gamma-ray irradiation.

We also observed hard X-ray excited luminescence in film (Fig. 6).[4,6] Films containing **P-dots** were prepared and their luminescence was measured. The photograph of the prepared films is shown in Fig. 7. A hard X-ray excited emission signal was observed for **P-dots (1)**, **P-dots (2)**, and **P-dots (3)**, and the luminescence spectra for **P-dots (1)** and **P-dots (2)** were recorded. **P-dots (3)** had a weak signal, and it was difficult to record the emission spectrum, probably because of the low sensitivity of the detector in the long wavelength region.

Luminescence from electron pulse excitation was observed. Nanosecond electron beams of 32 MeV were directly irradiated on the **P-dot** solutions (Fig. 8). The radio-luminescence from electron pulse excitation was observed using a 4K video camera and a spectrometer (Fig. 8a and b).[5] We clearly observed the three distinct of radio-luminescence colors. The emission maximum wavelength was 465, 545, and 615 nm for **P-dots (1)**,

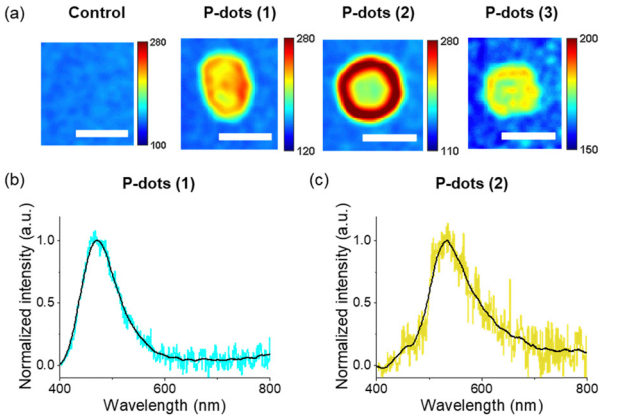

Fig. 6 (a) Hard X-ray excited radioluminescence on TADF **P-dots** film observed by a CCD camera, with the X-ray beam directed toward the **P-dots** films positioned approximately 30 cm below the X-ray aperture. All scale bars are 10 mm. (b) and (c) Scintillation emission spectra for **P-dots (1)** (b) and **P-dots (2)** (c), where each film sample was measured three times with an exposure time of 5 seconds per measurement for averaging. X-ray parameters for both experiments: 60 kVp and 40 mA, unfiltered for **P-dots (1)** (b) and **P-dots (2)** (c).

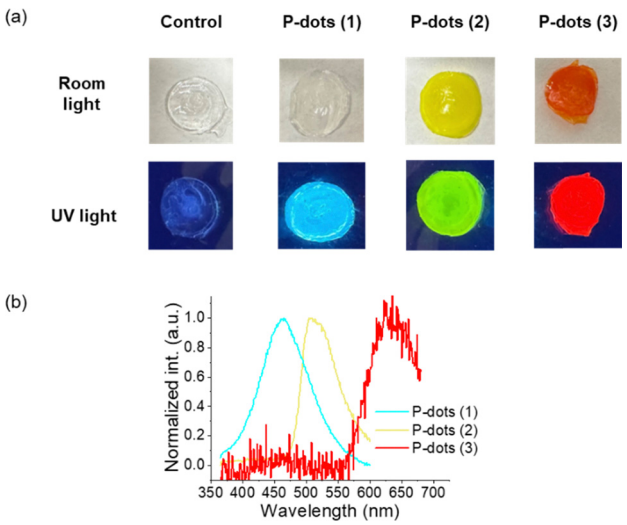

Fig. 7 (a) Photographs of films containing **P-dots** under room light (top) and under ultraviolet light (365 nm). (b) Photoluminescence spectra of films containing **P-dots** excited at 355 nm.

P-dots (2), and **P-dots (3)**, respectively, similar to that with UV excitation. The lower signal-to-noise ratio observed for **P-dot (3)** in Fig. 8 is primarily due to the inherently low quantum yield of its emission under UV excitation. This fundamental limitation reduces the overall emission intensity, leading to a decreased signal-to-noise ratio in the measurements. Regarding the secondary peak around 440 nm, we believe it arised from PVK.

In this study, we observed that various types of radiation (electron beam, hard X-ray and gamma-ray), responses against e-beam, X- and gamma-rays are the same. In X-ray and gamma-rays irradiation, many secondary excited electrons are generated, and these electrons cause luminescence (scintillation).[15]

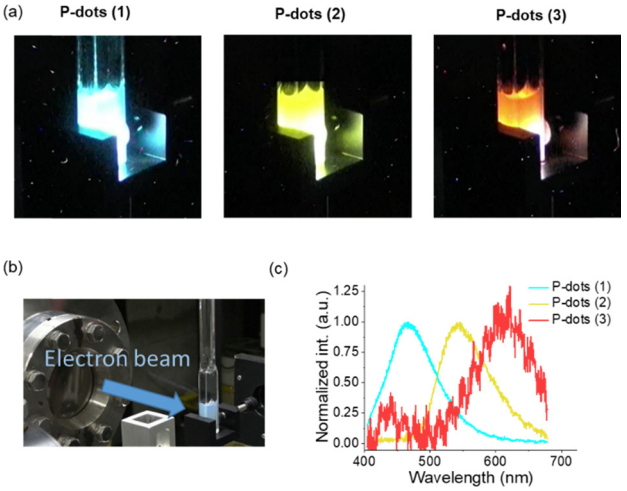

Fig. 8 Radio luminescence of **P-dots** observed by electron beam irradiation. (a) Photographs for **P-dots (1)**, **P-dots (2)**, and **P-dots (3)**. (b) The experimental setup photograph. (c) Radio-luminescence spectra for **P-dots (1)** (sky blue), **P-dots (2)** (yellow), and **P-dots (3)** (red).

Thus, we believe that they fundamentally show very similar responses. In addition, the various TADF **P-dots** show significant suppression of oxygen-induced quenching, indicating that it is important to consider the effect of oxygen on TADF scintillators as well, and providing a design guideline.[17] We have successfully observed scintillation with various types of radiation with the newly synthesized TADF **P-dots** in new colors and have examined this in detail.

Conclusions

In this study, we investigated the multicolor radio-luminescence of **P-dots** encapsulating three different TADF molecules. Electron beams, hard X-rays, and gamma rays were used to study the radiation excitation luminescence, and the photochemical properties were also thoroughly investigated. The new scintillator has succeeded in produced multi-color emission, which was previously limited to blue, and this is an important advance in the development of nano-sized emission scintillators for bio-imaging and sensing. These studies are expected to have a wide range of applications in the future, including in medical technology, biological research, and environmental monitoring.

Author contributions

Z. S., H. T. M. N., Z. L., D. A., M. Y., M. K., S. T., G. P., M. F. and Y. O. contributed to data acquisition. H. S., T. M., and T. K. contributed to PL lifetime measurements. M. F. and Y. O. supervised the project.

Data availability

A data availability statement (DAS) is required to be submitted alongside all articles. Please read our full guidance on data availability statements for more details and examples of suitable statements you can use.

Conflicts of interest

There are no conflicts to declare.

Acknowledgements

This work was partly supported by a Grant-in-Aid for Scientific Research (B) (No. JP23H01804 (Y. O.)), and trans-formative Research Areas (JP23H04906 (M. F.)). HTMN received funding through the Stanford Molecular Imaging Scholars (SMIS) Program, supported by NIH grant T32 CA118681. We thank Heather Fish, MChem, from Edanz (**https://jp.edanz.com/ac**) for editing a draft of this manuscript.

Notes and references

1 Y.-Z. Shi, H. Wu, K. Wang, J. Yu, X.-M. Ou and X.-H. Zhang, *Chem. Sci.*, 2022, **13**, 3625–3651.
2 M. A. Bryden and E. Zysman-Colman, *Chem. Soc. Rev.*, 2021, **50**, 7587–7680.
3 T. Li, D. Yang, L. Zhai, S. Wang, B. Zhao, N. Fu, L. Wang, Y. Tao and W. Huang, *Adv. Sci.*, 2017, **4**, 1600166.
4 Y. Osakada, G. Pratx, L. Hanson, P. E. Solomon, L. Xing and B. Cui, *Chem. Commun.*, 2013, **49**, 4319–4321.
5 Z. Liu, Z. Su, D. Asanuma, S. Tojo, M. Yamaji, M. Fujitsuka and Y. Osakada, *Photochem. Photobiol. Sci.*, 2024, **23**, 329–338.
6 Y. Osakada, G. Pratx, C. Sun, M. Sakamoto, M. Ahmad, O. Volotskova, Q. Ong, T. Teranishi, Y. Harada, L. Xing and B. Cui, *Chem. Commun.*, 2014, **50**, 3549–3551.
7 O. D. I. Moseley, T. A. S. Doherty, R. Parmee, M. Anaya and S. D. Stranks, *J. Mater. Chem. C*, 2021, **9**, 11588–11604.
8 W. Ma, Y. Su, Q. Zhang, C. Deng, L. Pasquali, W. Zhu, Y. Tian, P. Ran, Z. Chen and G. Yang, *Nat. Mater.*, 2022, **21**, 210–216.
9 S. Yuan, G. Zhang, F. Chen, J. Chen, Y. Zhang, Y. Di, Y. Chen, Y. Zhu, M. Lin and H. Chen, *Adv. Funct. Mater.*, 2024, 2400436.
10 H. Cui, W. Zhu, Y. Deng, T. Jiang, A. Yu, H. Chen, S. Liu and Q. Zhao, *Aggregate*, 2024, **5**, e454.
11 L. Lu, M. Sun, T. Wu, Q. Lu, B. Chen and B. Huang, *Nanoscale Adv.*, 2022, **4**, 680–696.
12 L. He, X. Yu and W. Li, *ACS Nano*, 2022, **16**, 19691–19721.
13 W. Ma, Y. Su, Q. Zhang, C. Deng, L. Pasquali, W. Zhu, Y. Tian, P. Ran, Z. Chen, G. Yang, G. Liang, T. Liu, H. Zhu, P. Huang, H. Zhong, K. Wang, S. Peng, J. Xia, H. Liu, X. Liu and Y. M. Yang, *Nat. Mater.*, 2022, **21**, 210–216.
14 J.-X. Wang, L. Gutiérrez-Arzaluz, X. Wang, T. He, Y. Zhang, M. Eddaoudi, O. M. Bakr and O. F. Mohammed, *Nat. Photonics*, 2022, **16**, 869–875.
15 T. Yanagida, *Proc. Jpn. Acad., Ser. B*, 2018, **94**, 75–97.
16 M. Koshimizu, *Jpn. J. Appl. Phys.*, 2023, **62**, 010503.

17 D. Asanuma, H. T. Minh Nguyen, Z. Liu, S. Tojo, H. Shigemitsu, M. Yamaji, K. Kawai, T. Mori, T. Kida, G. Pratx, M. Fujitsuka and Y. Osakada, *Nanoscale Adv.*, 2023, **5**, 3424–3427.
18 A. F. Bartley, M. Fischer, M. E. Bagley, J. A. Barnes, M. K. Burdette, K. E. Cannon, M. S. Bolding, S. H. Foulger, L. L. McMahon and J. P. Weick, *J. Neural Eng.*, 2021, **18**, 046036.
19 W. Yang, C. Xie, T. Chen, X. Yin, Q. Lin, S. Gong, Z. Quan and C. Yang, *Angew. Chem., Int. Ed.*, 2024, e202402704.
20 Q. Zhang, B. Li, S. Huang, H. Nomura, H. Tanaka and C. Adachi, *Nat. Photonics*, 2014, **8**, 326–332.
21 T.-Y. Shang, L.-H. Lu, Z. Cao, Y. Liu, W.-M. He and B. Yu, *Chem. Commun.*, 2019, **55**, 5408–5419.
22 J. X. Chen, Y. F. Xiao, K. Wang, D. Sun, X. C. Fan, X. Zhang, M. Zhang, Y. Z. Shi, J. Yu and F. X. Geng, *Angew. Chem., Int. Ed.*, 2021, **133**, 2508–2514.
23 E. Y. Park, J. H. Park, Y.-H. Kim and M. C. Suh, *J. Mater. Chem. C*, 2022, **10**, 4705–4716.
24 *Handbook of photochemistry*, ed., M. Montalti, A. Credi, L. Prodi, M. T. Gandolfi, 3rd edn, 2006.
25 T. Nakagawa, K. Okamoto, H. Hanada and R. Katoh, *Opt. Lett.*, 2016, **41**, 1498–1501.
26 N. Kawano, M. Koshimizu, G. Okada, Y. Fujimoto, N. Kawaguchi, T. Yanagida and K. Asai, *Sci. Rep.*, 2017, **7**, 14754.
27 L. M. Bollinger and G. E. Thomas, *Rev. Sci. Instrum.*, 1961, **32**, 1044–1050.

